Precisely measuring M_W at the LHC: estimating bottom quark effects and PDF uncertainties

Emanuele A. Bagnaschi

18 February 2022

CERN online

emanuele.bagnaschi@cern.ch

EB et al. JHEP 07 (2018) 101

EB and A. Vicini Phys.Rev.Lett. 126 (2021) 4, 041801

Introduction

The case for the W mass

- The M_W mass measurement is one of the important item of the SM precision program at the LHC.
- The value of M_W is important to understand the consistency of the SM and to constraint new physics.

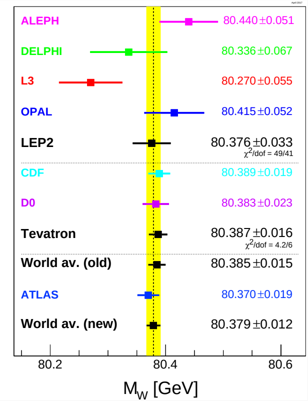

[PDG 2021]

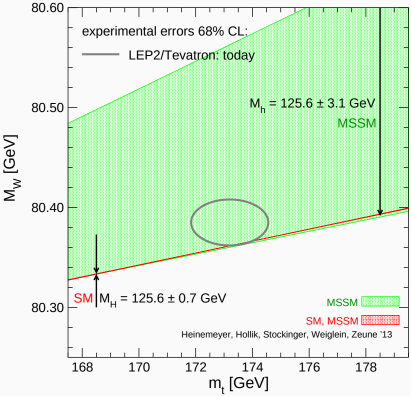

[1311.1663]

Link with another anomalies: M_W vs $(g-2)_\mu$

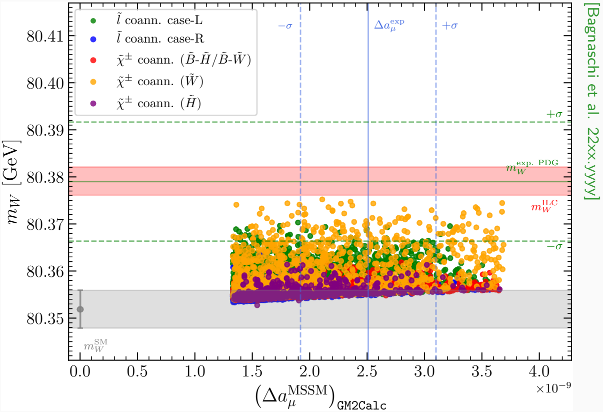

- There is a mild correlation between M_W and $(g-2)_\mu$, with interesting patterns arising in connection with DM mechanisms
- The MSSM covers well all the relevant range of Δa_μ
- For these scenarios, M_W is in general below the current exp. average, although many points lie within 1σ

Introduction

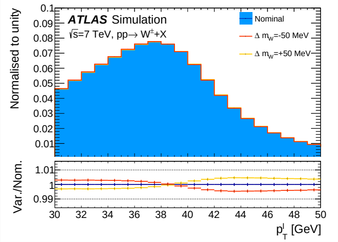

- The measurement of the W mass is performed using a template-fit approach.
- it depends on the theory models encoded in the tools (Monte Carlo event generators) used to produce the templates.
- One element that therefore enters these predictions is the *non-perturbative tune* of the Parton Shower (PS).

- To tune the PS, precisely measured observables are needed.
- A prime target is the transverse momentum distribution of the Z ($l\bar{l}$).

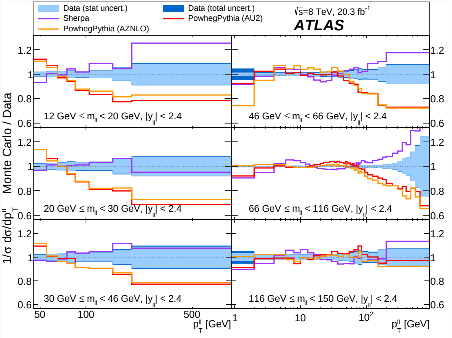

[ATLAS 1512.02192]

Introduction

- The PS non-perturbative tune adsorb in an effective way everything that has not been properly described by the theory prediction.

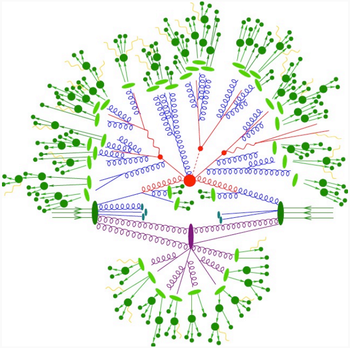

[SHERPA]

- One should strive to control as much as possible and leave in the tune only universal, non-perturbative effects.
- In the past few years, the question of how using a massless description for the bottom-quark induced contributions may/may not induce spurious *non-universal* terms to be included in the PS tune.
- Goal: build an improved description of the bottom-quark induced contribution to the Z transverse momentum.
- Other studies of mass quark effects in Drell-Yan recently published, [Pietrulewicz et al '17, Krauss et al' 17, Figueroa et al '18, Höeche et al. '19].

The process

$\bar{l}l + X$ production

- For a review of the recent results, see the talks of M. Wiesemann and F. Buccioni presented at the EW WG general meeting this week

QCD

- NNLO differential [Melnikov et al 06, Catani et al '09, Gavin et al '10 and '12]
- Resummation [Arnold et al '91, Balasz et al '95, Ellis et al '97, Qiu et al '00, Kulesza et al '01 and '02, Bozzi '10, Bizoń et al '18, Bizoń et al '19]
- NLO MC+PS [Frixione et al (MC@NLO), Alioli '08, Alwall et al '14, SHERPA]
- NNLO MC+PS [Höche et al '14, Karlberg et al '14, Frederix et al , Monni et al '19, '20, Alioli et al '21]
- N3LO [Duhr et al. '20, '21, Camarda et al. '21, Chen et al '21]

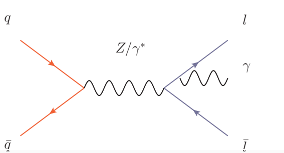

EW

- NLO EW [Baur et al '97-'04 , Brein et al '99, Dittmaier et al '01, Zykunov '01 and '05, Arbuzov et al '05 and '06, Carloni Calame et al '06 and '07, Brensing et al '07, Dittmaier et al '09]
- NLO QCD/EW + PS [Bernaciak et al, Barze et al '12 and '13, Mück et al '16]
- Mixed QCD-EW [Dittmaier et al '14 and '15, Buccioni et al '19, '20, '21, Bonciani et al. '20]

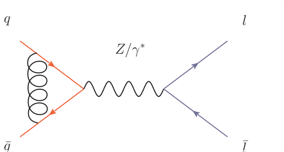

$l\bar{l} + X$ production: the 5FS

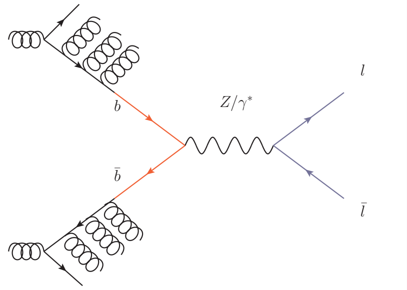

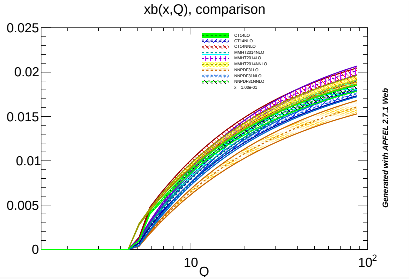

- Computation all in the 5FS, where the bottom is a massless initial state quark.
- DGLAP evolution of the bottom PDF resums large logs $\mathcal{O}(\log(m_Z/m_b))$.
- Neglects terms of order m_b/m_Z and less accurate description for kinematic distributions where the QCD radiation can be influenced by the natural mass scale of the bottom.

$\bar{l}l b\bar{b} + X$ production in the 4FS

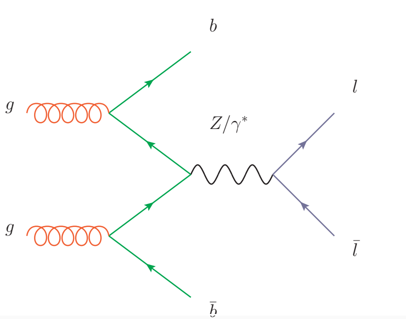

- In the 4FS the bottom quark is massive and no PDF is present in the proton.
- Collinear logs, which are resummed in the 5FS, are included only at FO in the 4FS.
- On the other hand, the terms of order m_b/m_Z are included.

QCD

- NLO-QCD: [J.M. Campbell and R.K. Ellis '06, Campbell et al. '03 and '06, Maltoni et al. '05, Febres Cordero et al. '08 and '09]

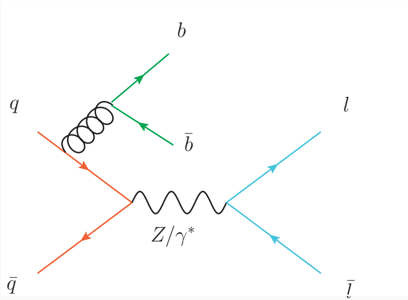

$\bar{l}lb\bar{b} + X$ production in the 4FS

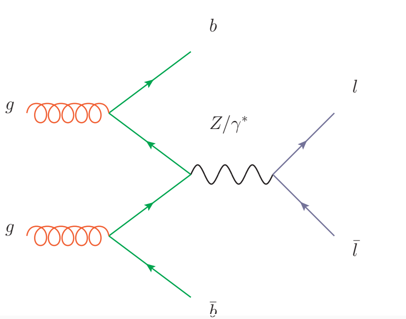

MC

- The process has been studied up to NLO-QCD+PS, using automated frameworks for the generation of the amplitudes. [Frederix et al '11, Krauss et al '16]

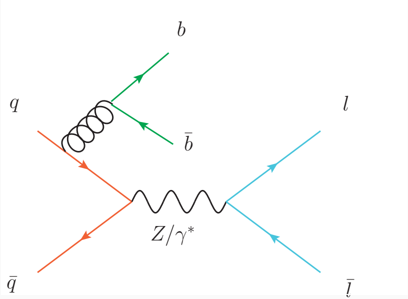

- In the 4FS the bottom quark is massive and no PDF is present in the proton.
- Collinear logs, which are resummed in the 5FS, are included only at FO in the 4FS.
- On the other hand, the terms of order m_b/m_Z are included.

The frameworks

We use implementations of the 5FS and 4FS process in the MG5_aMC@NLO and POWHEG-BOX NLO+PS frameworks. To generate the matrix elements, MadGraph and MadLoop were used in both cases

MC@NLO

$$\left(\frac{\mathrm{d}\sigma}{\mathrm{d}O}\right)_{\text{MC@NLO}} =$$
$$\sum_{n\geq 0}\int\left[B\otimes\Gamma+\hat{V}_{\text{fin}}\otimes\Gamma+\int\hat{R}^{s}_{\texttt{MC@NLO}}\otimes\Gamma\,\mathrm{d}\Phi_{r}^{\text{MC}}\right]\frac{\mathrm{d}\Phi_{B}\,\mathrm{d}\Phi_{n}^{\text{MC}}}{\mathrm{d}O}\,\mathcal{I}_{n}(t_1\equiv Q^{s}_{\text{sh}})$$
$$+\sum_{n\geq 1}\int\left[R\otimes\Gamma\,\frac{\mathrm{d}\Phi\,\mathrm{d}\Phi_{n-1}^{\text{MC}}}{\mathrm{d}O}-R^{s}_{\texttt{MC@NLO}}\otimes\Gamma\,\frac{\mathrm{d}\Phi^{\text{MC}}\,\mathrm{d}\Phi_{n-1}^{\text{MC}}}{\mathrm{d}O}\right]\mathcal{I}_{n-1}(t_1\equiv Q^{h}_{\text{sh}})$$

- Matching systematic estimated by varying the shower scale prescription (Sudakov form factor only from the PS).

The frameworks

We use implementations of the 5FS and 4FS process in the MG5_aMC@NLO and POWHEG-BOX NLO+PS frameworks. To generate the matrix elements, MadGraph and MadLoop were used in both cases

POWHEG

$$\left(\frac{\mathrm{d}\sigma}{\mathrm{d}O}\right)_{\mathtt{POWHEG}} = \sum_{n\geq 1}\int \left[\bar{B}^s\,\mathrm{d}\Phi_B \left\{\Delta^s_{t_{\min}} + \Delta^s_t \frac{R^s_{\mathtt{POWHEG}}}{B}\mathrm{d}\Phi_r\right\} + R^f_{\mathtt{POWHEG}} \otimes \Gamma\,\mathrm{d}\Phi \; + R_{\mathrm{reg}} \otimes \Gamma\,\mathrm{d}\Phi\right] \frac{\mathrm{d}\Phi^{\mathrm{MC}}_{n-1}}{\mathrm{d}O}\mathcal{I}_{n-1}(t_1 \equiv p_\perp^{\mathrm{rad}})$$

$$\overline{B}^s = B(\Phi_b) + \left[V(\Phi_b) + \int \mathrm{d}\Phi_{R|B}\hat{R}^s_{\mathtt{POWHEG}}(\Phi_{R|B})\right]$$

$$\Delta^s_t(\bar{\Phi}_B, p_T) = \exp\left\{-\int d\Phi_{\mathrm{rad}}\frac{R^s_{\mathtt{POWHEG}}(\bar{\Phi}_B, \Phi_{\mathrm{rad}})}{B(\Phi_1)}\theta(k_T - p_T)\right\}$$

$$R^s_{\mathtt{POWHEG}} = \frac{h^2}{h^2 + p_T^2}R \quad , \quad R^f_{\mathtt{POWHEG}} = \frac{p_T^2}{h^2 + p_T^2}R$$

- Matching systematic estimated by varying the value of the damping factor and the shower scale prescription.

Shower scale (SCALUP) prescriptions

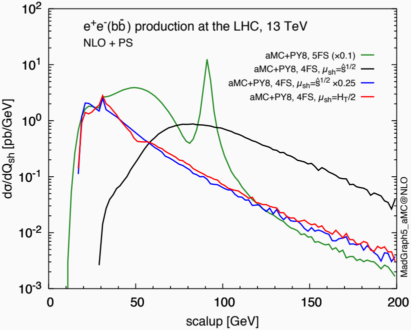

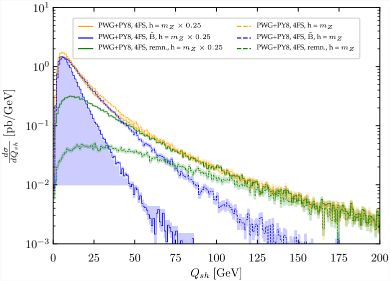

- Two different kinematic variables used to defined the shower scale distribution.
- For each one it is possible to apply "rescaling" factors.

- Two different event classes: $\tilde{B}$ and remnant.
- Shower scale for $\tilde{B}$ events is fixed by the `POWHEG` formalism.
- Shower scale for the remnant event can be modified from the default prescription (the p_T of the radiated parton). We apply a rescaling factor.

The setup

- LHC pp @ $\sqrt{S} = 13$ TeV.
- PDF, reference set: NNPDF3.0 ($n_f = 4$), $\alpha_S = 0.118$.
- μ_r and μ_f scale variation with a standard seven-combination prescription.
- MG5_aMC@NLO: two prescriptions for the extraction of the shower scale (H_T and $\hat{s}$).
- POWHEG-BOX: factor of $1/2$ variation for the shower scale of the remnant events.

Neutral-current Drell-Yan

- $\mu_r = \frac{1}{4}\sqrt{M(\bar{l}l)^2 + p_\perp(\bar{l}l)^2}$
- $\mu_f = \frac{1}{4}\sqrt{M(\bar{l}l)^2 + p_\perp(\bar{l}l)^2}$
- Gen. cuts: $M(\bar{l}l) > 30$ GeV
- Analysis cuts:
  1. $p_\perp(l/\bar{l}) > 20$ GeV
  2. $\eta(l/\bar{l}) < 2.5$
  3. $|M(\bar{l}l) - M_Z| < 15$ GeV

4FS $\bar{l}lb\bar{b}$

- $\mu_r = \frac{1}{4}\sqrt{M(\bar{l}l)^2 + p_\perp(\bar{l}l)^2}$
- $\mu_f = \frac{1}{4}\sqrt{M(\bar{l}l)^2 + p_\perp(\bar{l}l)^2}$
- Gen. cuts: $M(\bar{l}l) > 30$ GeV
- Analysis cuts:
  1. $p_\perp(l/\bar{l}) > 20$ GeV
  2. $\eta(l/\bar{l}) < 2.5$
  3. $|M(\bar{l}l) - M_Z| < 15$ GeV

Charged-current Drell-Yan

- $\mu_r = \sqrt{M(\bar{l}l)^2 + p_\perp(\bar{l}l)^2}$
- $\mu_f = \sqrt{M(\bar{l}l)^2 + p_\perp(\bar{l}l)^2}$
- Analysis cuts:
  1. $p_\perp(l^\pm/missing) >$ 25 GeV
  2. $\eta(l^\pm) < 2.5$

Results

5FS: the transverse momentum of the $\bar{l}l$ system

- Different initial state flavor contribute in a different way
- Bottom contribution peak shifted.
- Bottom: first bin kink due to PS when bottom quarks are involved.

initial state quark	cross section (pb)	%
u	245.54 ± 0.13	33.0
d	277.98 ± 0.14	37.4
c	63.86 ± 0.07	8.6
s	127.90 ± 0.09	17.2
b	28.31 ± 0.05	3.8
total	743.61 ± 0.22	100.0

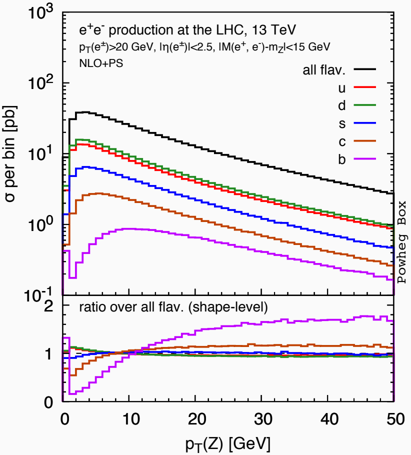

4FS: the transverse momentum of the $l\bar{l}b\bar{b}$ system

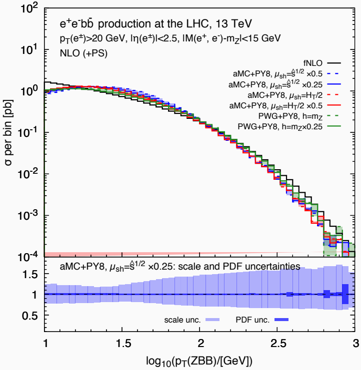

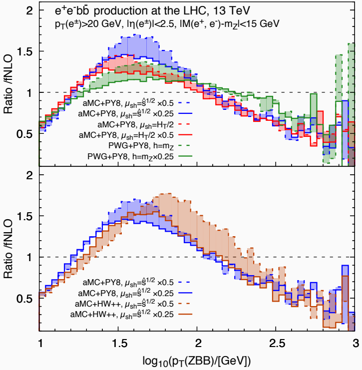

- LO system recoils against emitted parton; the p_T distribution is divergent at fixed order.
- Matching with PS cures the divergence.
- Maximum discrepancy between the frameworks in the intermediate region.
- Both MCs show a high-p_T tail below the fixed order.

4FS: Number of b-tagged jets

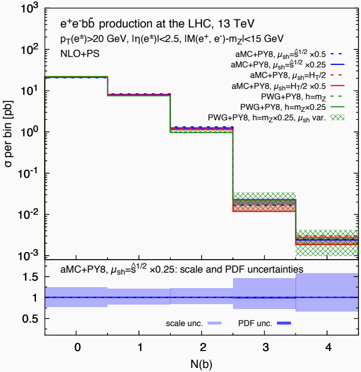

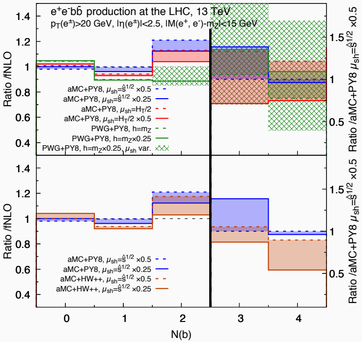

- B-jet definition: anti-K_T, $R = 0.4$, at least one b-hadron.
- B-jet cuts: $p_T(j) > 30$ GeV, $|\eta(j)| < 2.5$.
- Different behavior between the two MCs: in `POWHEG` suppression in the bjet=2 bin, in `MG5_aMC@NLO` enhancement.

4FS: p_T of the hardest b-jets

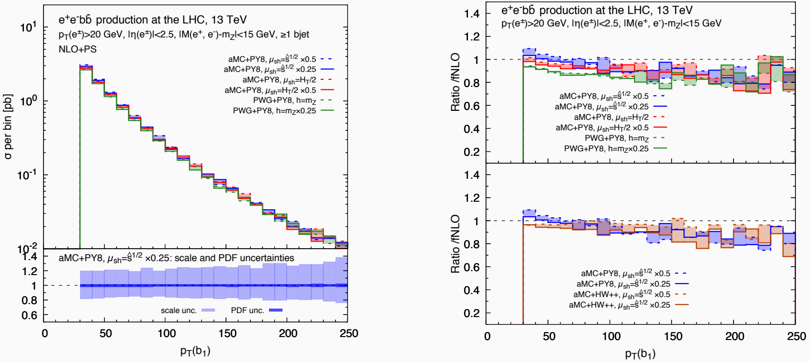

- 1st b-jet.
- Suppression of bjets rate in POWHEG w.r.t. to the NLO is manifest here.

4FS: p_T of the hardest b-jets

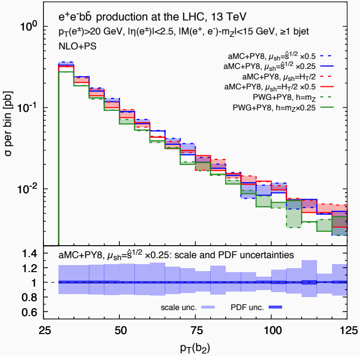

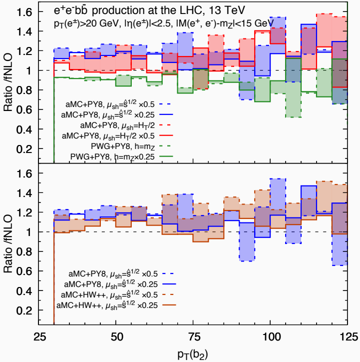

- 2nd b-jet.
- Suppression of bjets rate in POWHEG w.r.t. to the NLO is manifest here.

4FS: Invariant mass of the hardest b-hadrons

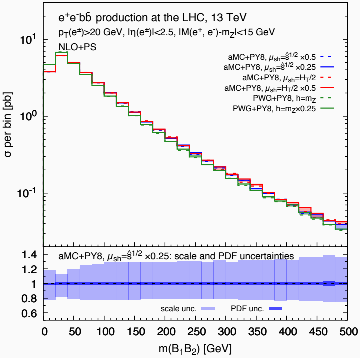

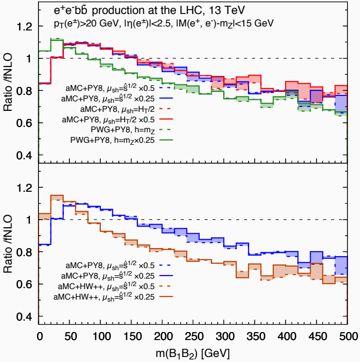

- no b-jet tagging.
- POWHEG peaks at lower masses than aMC@NLO+PY8, similarly to aMC@NLO+HW++.

4FS: Invariant mass of the hardest b-hadrons

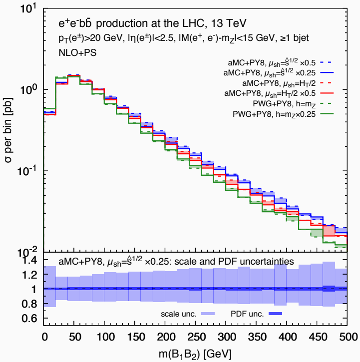

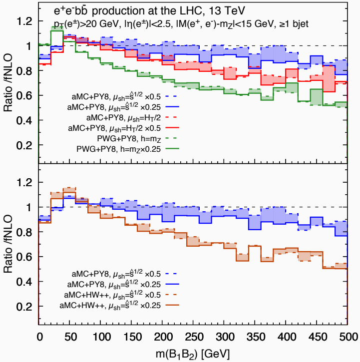

- 1 b-jet tagged.
- With one b-jet tagged, spread between the aMC@NLO predictions.

4FS: Invariant mass of the hardest b-hadrons

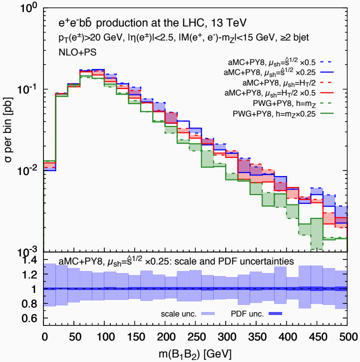

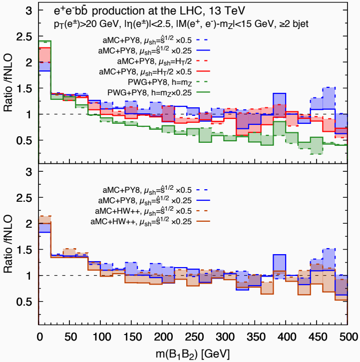

- 2 b-jet tagged.
- The difference becomes less prominent if we tag 2 b-jets.

4FS: separation of the hardest b-hadrons

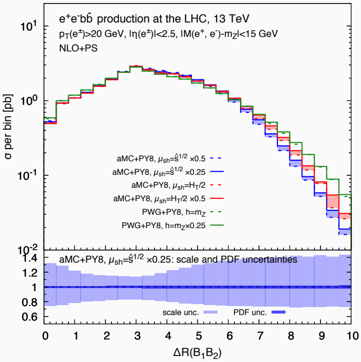

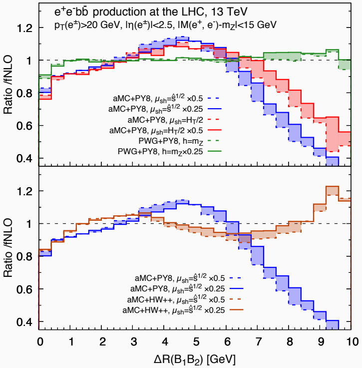

- no b-jet tagging.
- POWHEG closer to NLO than aMC@NLO.
- Great difference in aMC@NLO between the two showers, unless 2 b-jets tagged.
- Suppression of bjets rate in POWHEG w.r.t. to the NLO is manifest here.

4FS: separation of the hardest b-hadrons

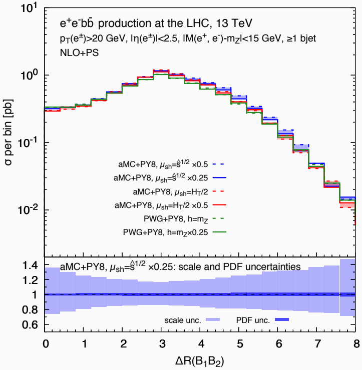

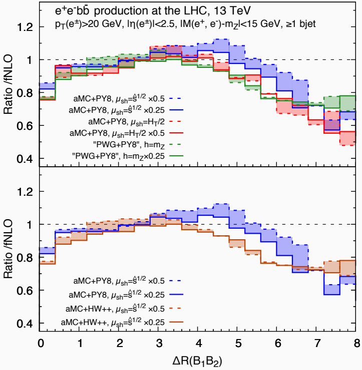

- 1 b-jet tagged.
- POWHEG closer to NLO than aMC@NLO.
- Great difference in aMC@NLO between the two showers, unless 2 b-jets tagged.
- Suppression of bjets rate in POWHEG w.r.t. to the NLO is manifest here.

4FS: separation of the hardest b-hadrons

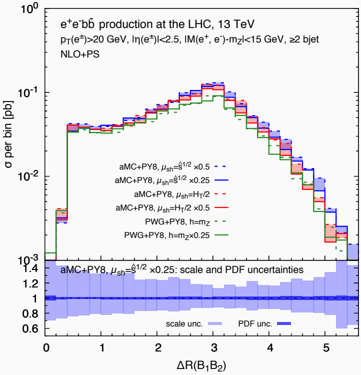

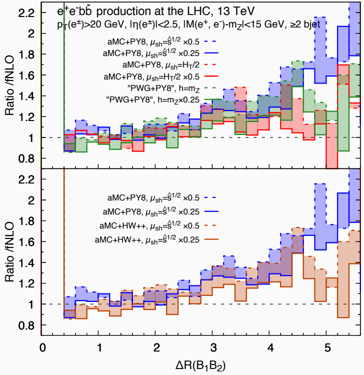

- 2 b-jet tagged.
- POWHEG closer to NLO than aMC@NLO.
- Great difference in aMC@NLO between the two showers, unless 2 b-jets tagged.
- Suppression of bjets rate in POWHEG w.r.t. to the NLO is manifest here.

4FS: the transverse momentum of the $\bar{l}l$ system

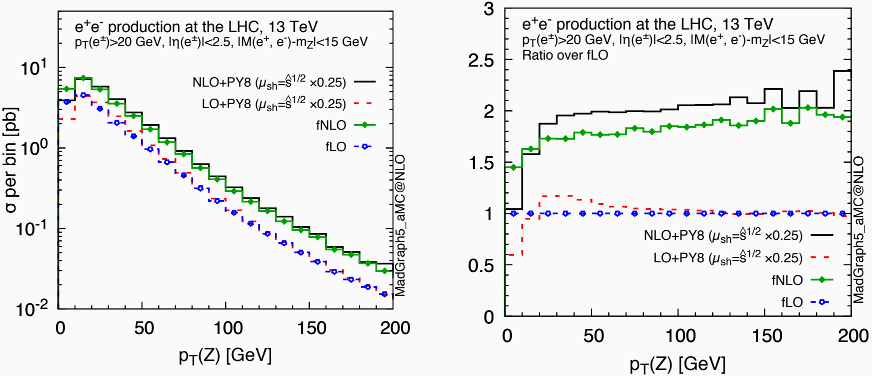

- Large differential NLO k-factor.
- Sizable effects from PS.

4FS: the transverse momentum of the $l\bar{l}$ system

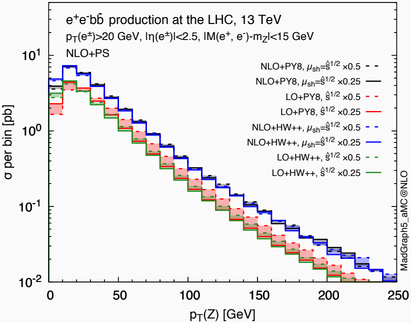

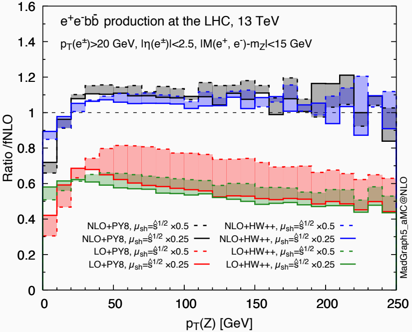

- Large differential NLO k-factor.
- Sizable effects from PS.

4FS: the transverse momentum of the $l\bar{l}$ system

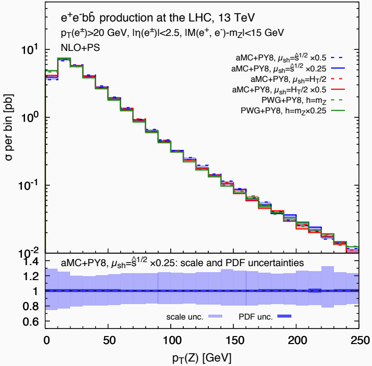

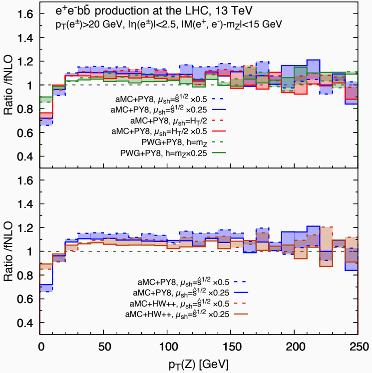

- PDF uncert. nearly constant, $\mathcal{O}(2\%)$; μ_r and μ_f scale dependence nearly constant, $\mathcal{O}(20\%)$.
- Matching uncertainty $\mathcal{O}(5\%)$ in both approaches.
- Larger differences between the two MCs and between PYTHIA8 and HERWIG++, especially in the first bins; non trivial dependence on p_T.

4FS: the transverse momentum of the $\bar{l}l$ system

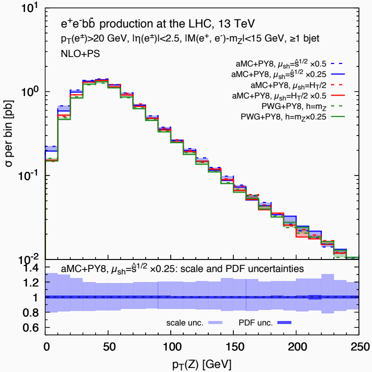

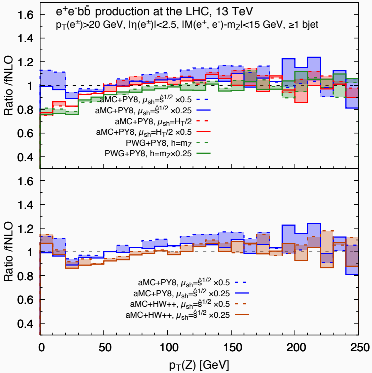

- PDF uncert. nearly constant, $\mathcal{O}(2\%)$; μ_r and μ_f scale dependence nearly constant, $\mathcal{O}(20\%)$.
- Matching uncertainty $\mathcal{O}(5\%)$ in both approaches.
- Larger differences between the two MCs and between PYTHIA8 and HERWIG++, especially in the first bins; non trivial dependence on p_T.

4FS: the transverse momentum of the $l\bar{l}$ system

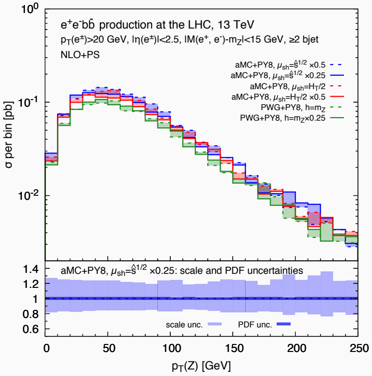

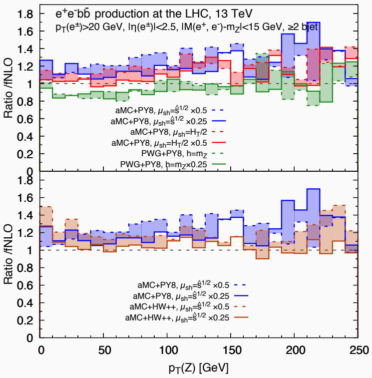

- PDF uncert. nearly constant, $\mathcal{O}(2\%)$; μ_r and μ_f scale dependence nearly constant, $\mathcal{O}(20\%)$.
- Matching uncertainty $\mathcal{O}(5\%)$ in both approaches.
- Larger differences between the two MCs and between PYTHIA8 and HERWIG++, especially in the first bins; non trivial dependence on p_T.

An improved prediction of $p_T^{l\bar{l}}$

- Goal: combine the two predictions in a consistent approach, avoiding double counting.

5FS

- B-hadrons from the PS in two cases:
    1. $b\bar{b}$ and bg channels: splitting in the backward evolution (no bottom content in the proton).
    2. For the other channel: $g \to b\bar{b}$ splitting.
- *We remove the bottom contribution by vetoing B-hadrons in final state.*

4FS

- By construction the process contains two massive bottom in the final state.
- Other bottoms will arise from PS splitting.
- Improved description which keeps into account the mass of the quark.

$$\frac{d\sigma^{\mathrm{best}}}{dp_\perp^{l^+l^-}} = \frac{d\sigma^{\mathrm{5FS-Bveto}}}{dp_\perp^{l^+l^-}} + \frac{d\sigma^{\mathrm{4FS}}}{dp_\perp^{l^+l^-}}$$

An improved prediction of $p_T^{l\bar{l}}$

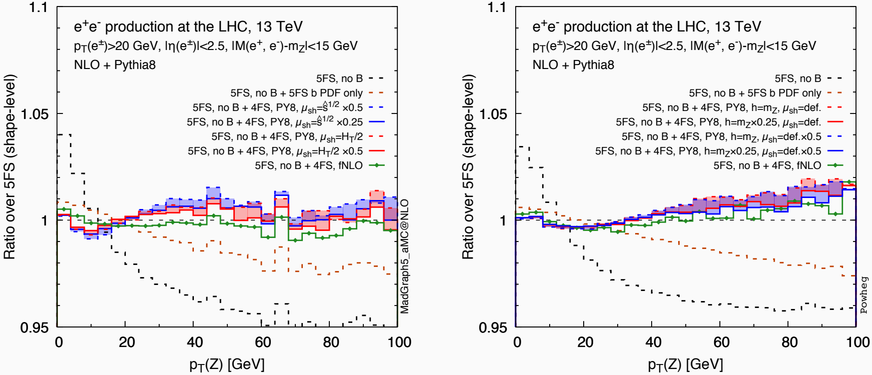

- 5FS b-contribution: non-trivial shape, the two contributions are of the same order of magnitude at large p_T, while at low p_t gluon splitting from light-quark induced processes dominates.
- Non-trivial shape distortion.
- Effects after merging of the order of $\mathcal{O}(\pm 1\%)$ for `MG5_aMC@NLO`, $\mathcal{O}(\pm 0.5\%)$.

An improved prediction of $p_T^{l\bar{l}}$

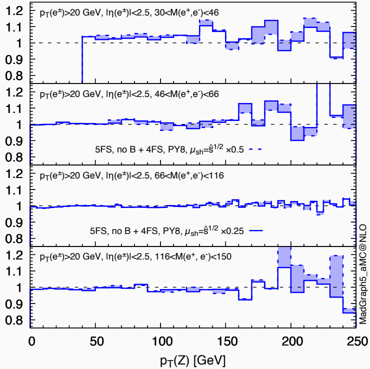

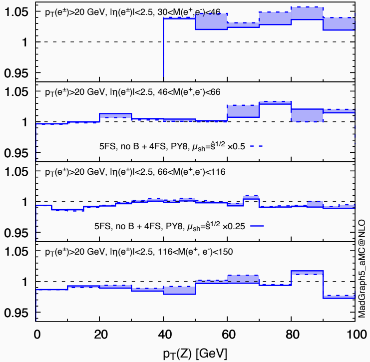

- Can we explain the difference in shape in observed spectrum vs the current MC samples? No.
- No sizable dependence on the invariant mass of the lepton pair.

An improved prediction of $p_T^{l\bar{l}}$

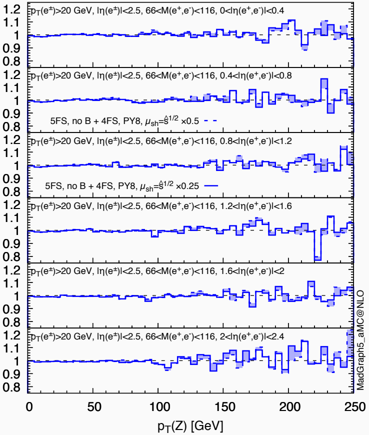

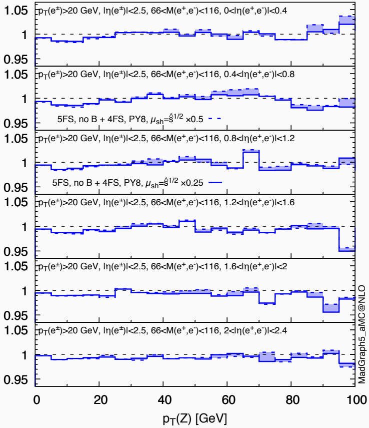

- Can we explain the difference in shape in observed spectrum vs the current MC samples? No.
- No sizable dependence on the pseudorapidity of the lepton pair.

The reweighting function

The canonical way to include these effects is to re-tune the parton shower MCs on the Z data using this improved prediction. To estimate these effects without performing the tune, we adopt the following procedure:

1. Define:

$$\mathcal{R}(p_\perp^{l^+l^-}) \equiv \left(\frac{1}{\sigma_{fid}^{best}} \frac{d\sigma^{best}}{dp_\perp^{l^+l^-}} \bigg|_{tuneX} \right) \cdot \left(\frac{1}{\sigma_{fid}^{5FS}} \frac{d\sigma^{5FS}}{dp_\perp^{l^+l^-}} \bigg|_{tuneX} \right)^{-1}$$

2. Suppose that we have two PS tunes called `tune1` which describe the data:

$$\frac{1}{\sigma_{fid}^{exp}} \frac{d\sigma^{exp}}{dp_\perp^{l^+l^-}} = \frac{1}{\sigma_{fid}^{5FS}} \frac{d\sigma^{5FS}}{dp_\perp^{l^+l^-}} \bigg|_{\mathtt{tune1}} = \frac{1}{\sigma_{fid}^{best}} \frac{d\sigma^{best}}{dp_\perp^{l^+l^-}} \bigg|_{\mathtt{tune2}} = \mathcal{R}(p_\perp^{l^+l^-}) \frac{1}{\sigma_{fid}^{5FS}} \frac{d\sigma^{5FS}}{dp_\perp^{l^+l^-}} \bigg|_{\mathtt{tune2}} .$$

3. From 1.+2. it follows that:

$$\frac{1}{\sigma_{fid}^{5FS}} \frac{d\sigma^{5FS}}{dp_\perp^{l^+l^-}} \bigg|_{\mathtt{tune2}} = \frac{1}{\mathcal{R}(p_\perp^{l^+l^-})} \frac{1}{\sigma_{fid}^{5FS}} \frac{d\sigma^{5FS}}{dp_\perp^{l^+l^-}} \bigg|_{\mathtt{tune1}} .$$

Impact on the W mass measurement

Measuring the W mass at the LHC

Three observables sensitive to the W mass: p_T^l, M_T^W, $p_T(missing)$.

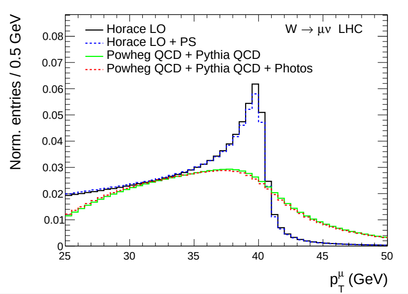

- High sensitivity to radiative corrections.
- Detector modeling under control.
- Peak around $m_W/2$.

[Carloni Calame et al '16]

W-boson charge	W^+		W^-		Combined	
Kinematic distribution	p_T^ℓ	m_T	p_T^ℓ	m_T	p_T^ℓ	m_T
δm_W [MeV]						
$\langle\mu\rangle$ scale factor	0.2	1.0	0.2	1.0	0.2	1.0
$\Sigma\bar{E}_T$ correction	0.9	12.2	1.1	10.2	1.0	11.2
Residual corrections (statistics)	2.0	2.7	2.0	2.7	2.0	2.7
Residual corrections (interpolation)	1.4	3.1	1.4	3.1	1.4	3.1
Residual corrections ($Z \to W$ extrapolation)	0.2	5.8	0.2	4.3	0.2	5.1
Total	2.6	14.2	2.7	11.8	2.6	13.0

[ATLAS 1701.07240]

Measuring the W mass at the LHC

Three observables sensitive to the W mass: p_T^l, M_T^W, $p_T(missing)$.

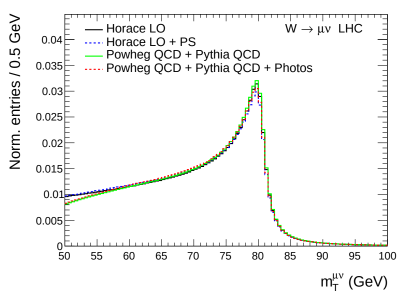

- $M_T = \sqrt{2 p_T^l p_T^{miss}(1 - \cos\ \Delta\phi)}$
- Stability under radiative corrections.
- Suffer from pileup and detector effects since it relies on $\not{E}_T$.
- Peak around m_W.

[Carloni Calame et al '16]

W-boson charge	W^+		W^-		Combined	
Kinematic distribution	p_T^ℓ	m_T	p_T^ℓ	m_T	p_T^ℓ	m_T
δm_W [MeV]						
$\langle\mu\rangle$ scale factor	0.2	1.0	0.2	1.0	0.2	1.0
$\Sigma\bar{E}_T$ correction	0.9	12.2	1.1	10.2	1.0	11.2
Residual corrections (statistics)	2.0	2.7	2.0	2.7	2.0	2.7
Residual corrections (interpolation)	1.4	3.1	1.4	3.1	1.4	3.1
Residual corrections ($Z \to W$ extrapolation)	0.2	5.8	0.2	4.3	0.2	5.1
Total	2.6	14.2	2.7	11.8	2.6	13.0

[ATLAS 1701.07240]

Current status of the theory uncertainty

Combined categories	Value [MeV]	Stat. Unc.	Muon Unc.	Elec. Unc.	Recoil Unc.	Bckg. Unc.	QCD Unc.	EW Unc.	PDF Unc.	Total Unc.	χ^2/dof of Comb.
m_T, W^+, e-μ	80370.0	12.3	8.3	6.7	14.5	9.7	9.4	3.4	16.9	30.9	2/6
m_T, W^-, e-μ	80381.1	13.9	8.8	6.6	11.8	10.2	9.7	3.4	16.2	30.5	7/6
m_T, $W^\pm$, e-μ	80375.7	9.6	7.8	5.5	13.0	8.3	9.6	3.4	10.2	25.1	11/13
p_T^ℓ, W^+, e-μ	80352.0	9.6	6.5	8.4	2.5	5.2	8.3	5.7	14.5	23.5	5/6
p_T^ℓ, W^-, e-μ	80383.4	10.8	7.0	8.1	2.5	6.1	8.1	5.7	13.5	23.6	10/6
p_T^ℓ, $W^\pm$, e-μ	80369.4	7.2	6.3	6.7	2.5	4.6	8.3	5.7	9.0	18.7	19/13
p_T^ℓ, $W^\pm$, e	80347.2	9.9	0.0	14.8	2.6	5.7	8.2	5.3	8.9	23.1	4/5
m_T, $W^\pm$, e	80364.6	13.5	0.0	14.4	13.2	12.8	9.5	3.4	10.2	30.8	8/5
m_T-p_T^ℓ, W^+, e	80345.4	11.7	0.0	16.0	3.8	7.4	8.3	5.0	13.7	27.4	1/5
m_T-p_T^ℓ, W^-, e	80359.4	12.9	0.0	15.1	3.9	8.5	8.4	4.9	13.4	27.6	8/5

$$
\begin{aligned}
m_W &= 80369.5 \pm 6.8\,\text{MeV(stat.)} \pm 10.6\,\text{MeV(exp. syst.)} \pm 13.6\,\text{MeV(mod. syst.)} \\
&= 80369.5 \pm 18.5\,\text{MeV},
\end{aligned}
$$

[ATLAS 1701.07240]

- Estimation provided by ATLAS.
- We want to use our improved prediction to estimate the uncertainty from heavy flavors.

The templates

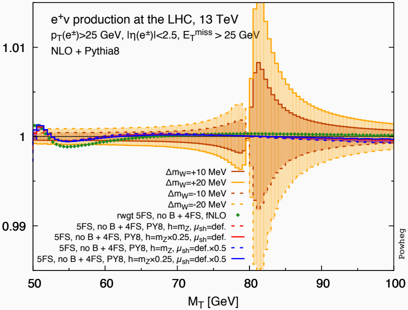

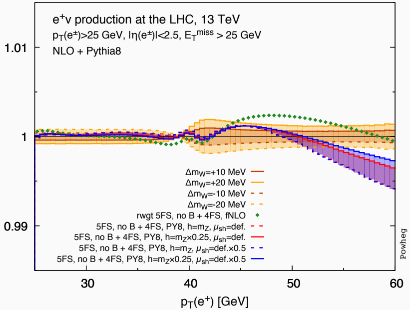

- Templates generation with both the POWHEG-BOX and MG5_aMC@NLO at NLO+PS in the 5FS.
- Different shape of the Jacobian peak for $p_T^{l^\pm}$ in the two Monte Carlos.
- Largest effects from the reweighting outside the canonical fit window.

The templates

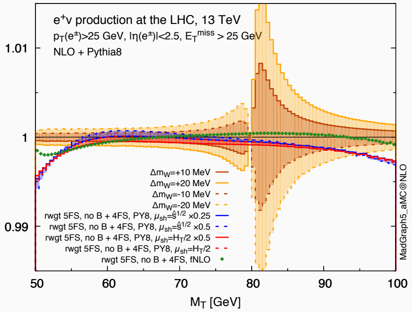

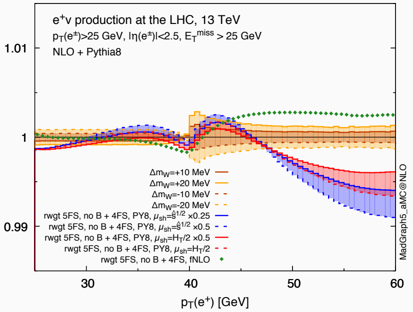

- Templates generation with both the `POWHEG-BOX` and `MG5_aMC@NLO` at NLO+PS in the 5FS.
- Different shape of the Jacobian peak for $p_T^{l^\pm}$ in the two Monte Carlos.
- Largest effects from the reweighting outside the canonical fit window.

Shift on the W mass measurement

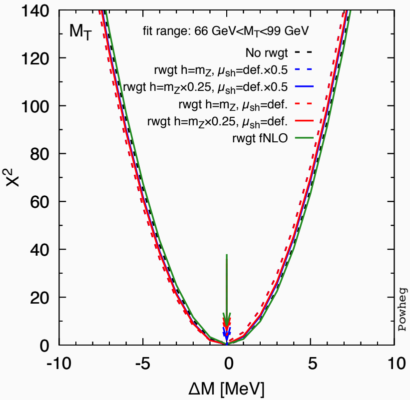

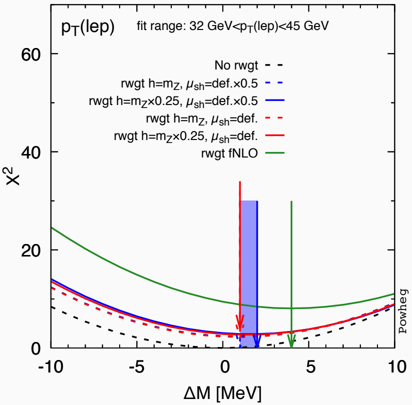

- Granularity of 1 MeV.
- Positive sign shift, at most reaching +5 MeV.
- Quite similar effect in POWHEG-BOX and in MG5_aMC@NLO.

Shift on the W mass measurement

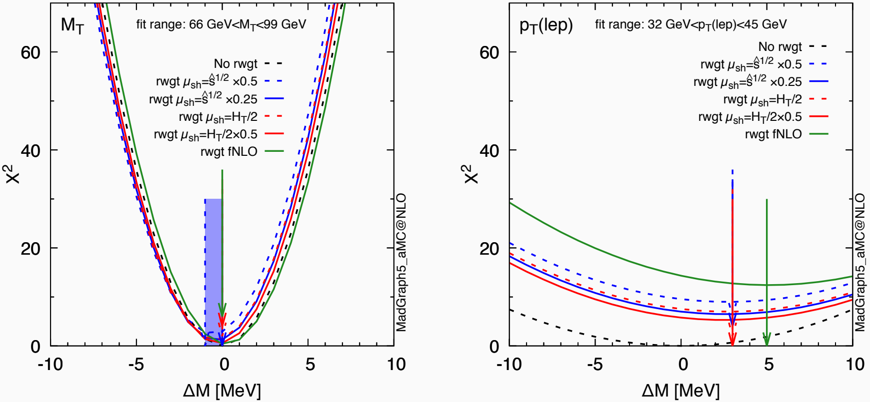

- Granularity of 1 MeV.
- Positive sign shift, at most reaching +5 MeV.
- Quite similar effect in POWHEG-BOX and in MG5_aMC@NLO.

Dependence of the shift on the fit window

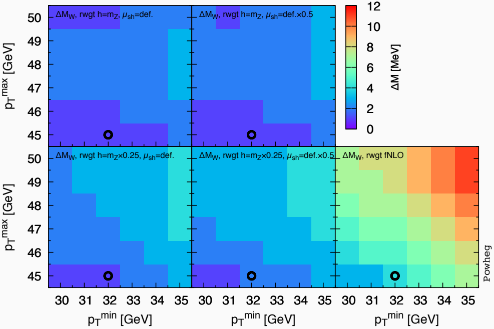

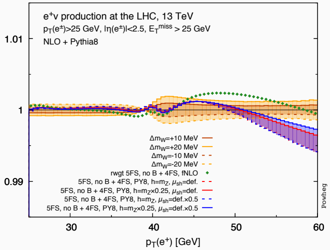

- Non-negligible dependence on the fit window due to the non-trivial shape of the reweighting function.

Dependence of the shift on the fit window

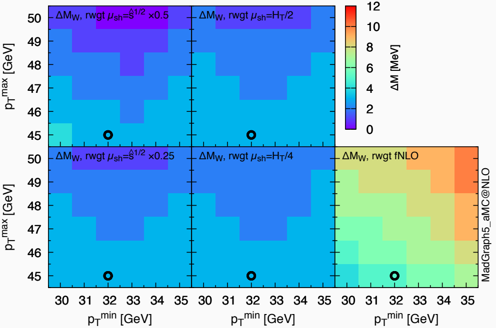

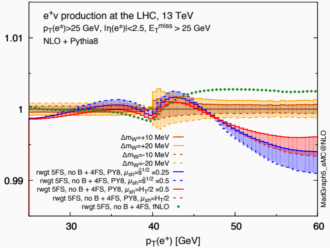

- Non-negligible dependence on the fit window due to the non-trivial shape of the reweighting function.

Conclusions

Summary and perspectives

The $\bar{l}lb\bar{b}$ process

- Multiscale process due to the presence of massive colored final states (the two bottom quarks).
- An accurate study of matching systematic shows sizable dependence on scheme/shower.
- Future: improved matching scheme needed to account for all the scales?

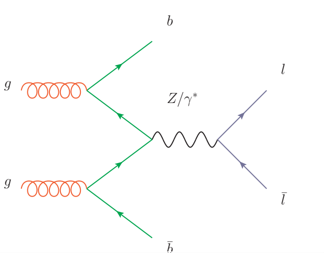

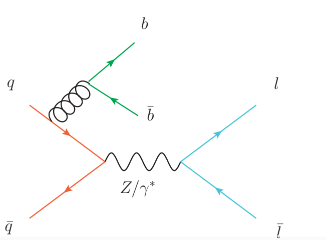

Summary and perspectives

W mass

- We have estimated the impact of including an improved description of the bottom induced contribution on the $l\bar{l}$ spectrum with respect to the standard 5FS description.
- The impact of these effects are estimated to be at most of of $\mathcal{O}(5 \text{ MeV})$.
- Future: Study how the picture changes using the same approach to generate the reweighting function but one order higher in the 5FS description, using DY-NNLOPS.
- Future: Understand the differences in the p_T^l templates between the POWHEG-BOX and MG5_aMC@NLO.

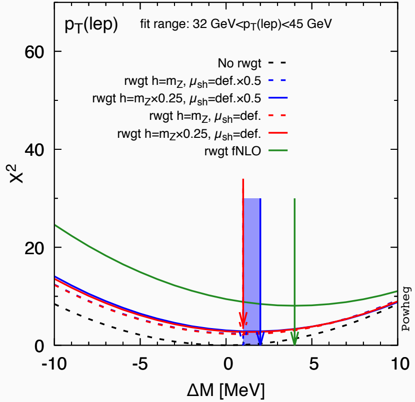

PDF uncertainties and the measurement of M_W at the LHC

Introduction and motivations

- Study the role of bin-bin correlations in the procedure used to estimate/include PDF uncertainty in the extraction of M_W at the LHC, with a specific focus on the long term perspectives.
- Three sets of uncertainties linked to PDFs:
  1. Uncertainty in the PDFs from the experimental uncertainty of the dataset used in the fit.
  2. Different fit methodologies (i.e. differences between PDF sets of different collaborations).
  3. Theoretical uncertainties of the predictions used in PDF fits. Concerning Missing Higher Order Uncertainties (MHOUs), their inclusion is starting to be addressed systematically only recently ([L. A. Harland-Lang, R. S. Thorne – 1811.08434], [R. A. Khalek et al. (NNPDF) – 1906.10698]).

Measuring the W mass at the LHC

Three observables sensitive to the W mass: M_T^W, $p_\perp^l$, $p_T(missing)$.

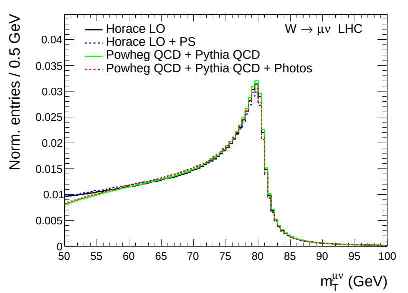

- Peak around m_W.
- $M_T = \sqrt{2 p_T^l p_T^{miss}(1 - \cos\ \Delta\phi)}$
- Suffer from pileup and detector effects since it relies on $\not{E}_T$.
- Stability under QCD radiative corrections.

[Carloni Calame et al '16]

W-boson charge	W^+		W^-		Combined	
Kinematic distribution	p_T^ℓ	m_T	p_T^ℓ	m_T	p_T^ℓ	m_T
δm_W [MeV]						
$\langle\mu\rangle$ scale factor	0.2	1.0	0.2	1.0	0.2	1.0
$\Sigma\bar{E}_T$ correction	0.9	12.2	1.1	10.2	1.0	11.2
Residual corrections (statistics)	2.0	2.7	2.0	2.7	2.0	2.7
Residual corrections (interpolation)	1.4	3.1	1.4	3.1	1.4	3.1
Residual corrections ($Z \to W$ extrapolation)	0.2	5.8	0.2	4.3	0.2	5.1
Total	2.6	14.2	2.7	11.8	2.6	13.0

[ATLAS 1701.07240]

Measuring the W mass at the LHC

Three observables sensitive to the W mass: M_T^W, $p_\perp^l$, $p_T(missing)$.

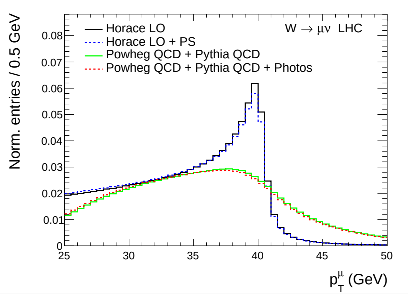

- Peak around $m_W/2$.
- Detector modeling under control.w
- High sensitivity to radiative corrections.
- We focus on $p_\perp^l$.

[Carloni Calame et al '16]

W-boson charge	W^+		W^-		Combined	
Kinematic distribution	p_T^ℓ	m_T	p_T^ℓ	m_T	p_T^ℓ	m_T
δm_W [MeV]						
$\langle\mu\rangle$ scale factor	0.2	1.0	0.2	1.0	0.2	1.0
$\Sigma\bar{E}_T$ correction	0.9	12.2	1.1	10.2	1.0	11.2
Residual corrections (statistics)	2.0	2.7	2.0	2.7	2.0	2.7
Residual corrections (interpolation)	1.4	3.1	1.4	3.1	1.4	3.1
Residual corrections ($Z \to W$ extrapolation)	0.2	5.8	0.2	4.3	0.2	5.1
Total	2.6	14.2	2.7	11.8	2.6	13.0

[ATLAS 1701.07240]

The study

Monte-Carlo setup

- W^+ generated with `POWHEG-BOX-v2 W_ew-BMNNP`, $\sqrt{S} = 13$ TeV, $\mu_r = \mu_f = m_W$.
- Accuracy: NLO-QCD+PS, showered with `PYTHIA82`.
- Cuts: $|\eta_l| < 2.5$, $p_l > 25$ GeV, $\not{E}_T > 25$ GeV.
- 15 million events; reweighted to the full set of 1000 replicae of `NNPDF30-1000`.

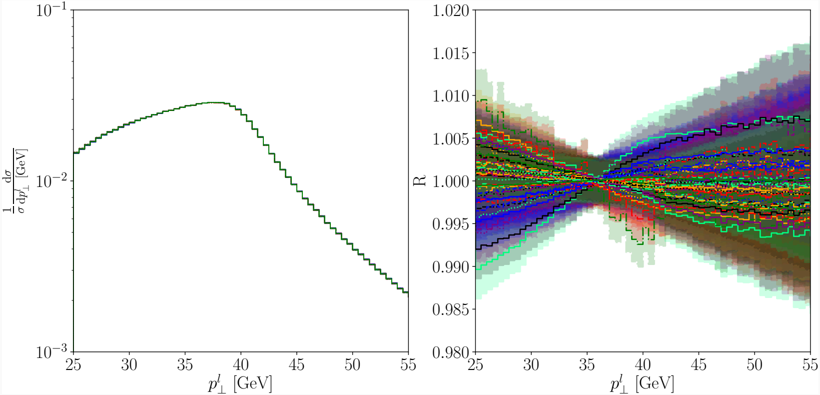

Previous studies for M_W

- Tevatron collaborations [0707.0085,0708.3642,0908.0766,1203.0275,1203.0293,1307.7627].
- Comprehensive study on the PDF uncertainty on M_T^W using modern matched MCs (see also [Bozzi, Rojo, Vicini – 1104.2056]), however with inaccurate M_T^W modeling.
- Subsequent study on p_T^l presented in [Bozzi, Citelli, Vicini – 1501.05587] and extended to the study of a high-rapidity lepton in [Bozzi, Citelli, Vesterinen, Vicini – 1508.06954].

Prescription for the estimation of the uncertainty in those studies

- Generate M_W-templates using the central replica of the NNPDF set.
- $\chi^2_{k,r} = \sum_{i \in bins} (\mathcal{T}_{0,k} - \mathcal{D}_r)^2_i / \sigma^2_i$.
- Fit other NNPDF replicae; compute the standard deviation of the M_W corresponding to minima of the replica χ^2 and take it as a proxy of the PDF uncertainty.
- Neglect the value of the χ^2.
- Fixed fit range, $p^l_\perp \in [29, 49]$ GeV.

- ATLAS [1701.07240], [Kotwal PRD 98, 033008].
- Other recent studies: [E. Manca, O. Cerri, N. Foppiani, L. Rolandi – 1707.09344], [L. Bianchini and G. Rolandi – 1902.03028], [S. Farry, O. Lupton, M. Pili, M. Vesterinen – 1902.04323], [M. Hussein, J. Isaacson, J. Huston – 1905.00110].

The role of bin-bin PDF correlations

Experimental side

- They were *not* included in the published M_W measurement from ATLAS, though the effect has been partially included through the combination of different categories.
- They will be included in future measurements both from ATLAS and CMS.
- They were included in other measurements (e.g. $\sin^2\theta_l^{eff}$, or α_s).

Phenomenological studies

- Included in the recent [S. Farry, O. Lupton, M. Pili, M. Vesterinen – 1902.04323], through a Bayesian reweighting procedure.

- What is the structure and origin of the bin-bin p_T^l correlations?
- What is the perspective for a measurement with a large integrated luminosity?

$p_\perp^l$ and PDF correlations

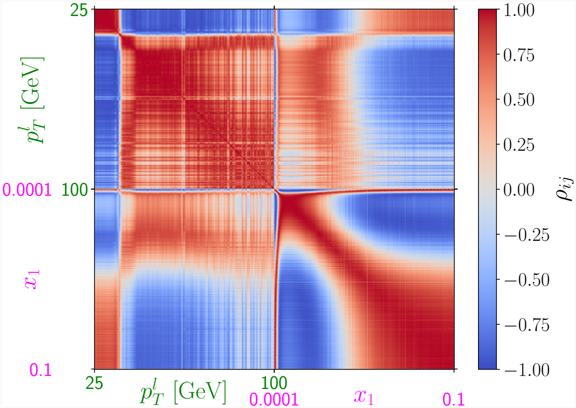

- Different elements drive correlation between replicae (QCD framework)
- $(\Sigma_{PDF})_{rs} \;=\; \langle(\mathcal{T}-\langle\mathcal{T}\rangle_{PDF})_r(\mathcal{T}-\langle\mathcal{T}\rangle_{PDF})_s\rangle_{PDF}$
- Block-structure in the $p_\perp^l$ self-correlation (top-left corner).
- Interplay in the hadron level cross-section between the parton-level cross-section and the luminosity.

Other observables

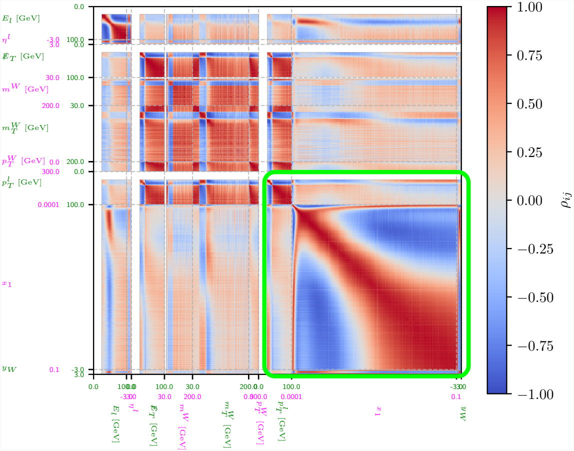

(caveat: *only* this plot at NNPDF30-100/LHEF)

- Shapes of differential observables non-trivially correlated under PDF variation

Fitting methodology

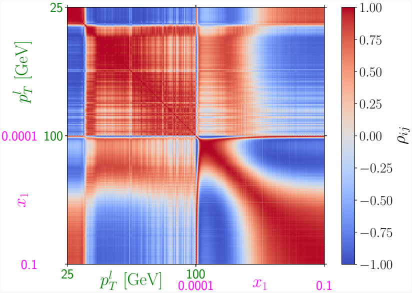

$$\chi^2_{k,min} = \sum_{(r,s)\in bins} (\mathcal{T}_{0,k} - \mathcal{D}^{exp})_r \left(C^{-1}\right)_{rs} (\mathcal{T}_{0,k} - \mathcal{D}^{exp})_s$$

$$C = \Sigma_{PDF} + \Sigma_{stat} + \Sigma_{MC} + \Sigma_{exp,syst}$$

$$(\Sigma_{PDF})_{rs} = \langle (\mathcal{T} - \langle \mathcal{T} \rangle_{PDF})_r (\mathcal{T} - \langle \mathcal{T} \rangle_{PDF})_s \rangle_{PDF}$$

$$\langle \mathcal{O} \rangle_{PDF} \equiv \frac{1}{N_{cov}} \sum_{l=1}^{N_{cov}} \mathcal{O}^{(l)}$$

- Fit the (pseudo)data using the templates (in our case the central replica in both cases), introducing a covariance matrix in the χ^2 definition.
- Estimate the PDF uncertainty as the half-width of the $\Delta\chi^2 = 1, 4, 9$ interval.
- The covariance matrix shows a non-trivial structure that has an impact in reducing the sensitivity to the PDF in the fit.

Results

Numerical results: without any covariance

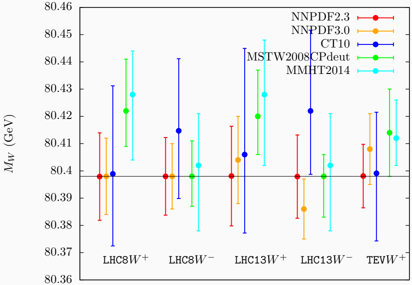

Fig. 4 left from [BCV - 1501.05587]

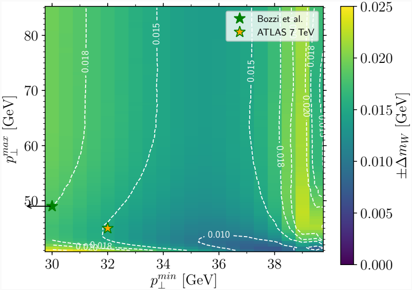

- $\chi^2_{k,r} = \sum_{i\in bins}(\mathcal{T}_{0,k} - \mathcal{D}_r)^2_i/\sigma^2_i$.
- Compatible results for (nearly) the same fit window.
- The study shows a sizable variability on the fit range.

Numerical results: with stat+PDF covariance

- PDF covariance + 1fb^{-1} stat. included.

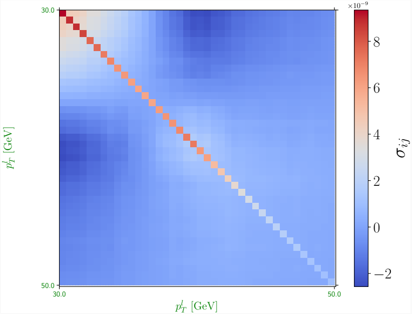

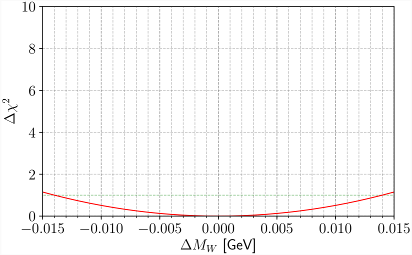

-

$$\chi^2_{k,min} = \sum_{(r,s)\in bins} (\mathcal{T}_{0,k} - \mathcal{D}^{exp})_r \left(C^{-1}\right)_{rs} (\mathcal{T}_{0,k} - \mathcal{D}^{exp})_s$$

$$C = \Sigma_{PDF} + \Sigma_{stat}$$

Numerical results: with stat+PDF covariance

- PDF covariance + 300fb^{-1} stat. included.

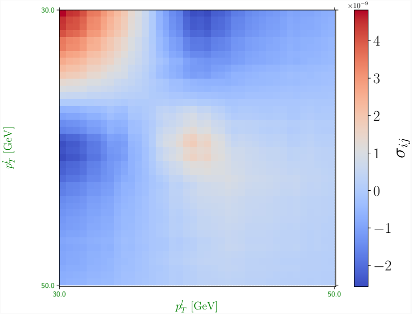

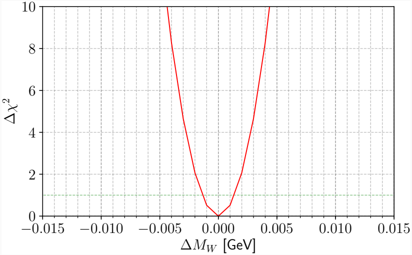

-

$$\chi^2_{k,min} = \sum_{(r,s)\in bins} (\mathcal{T}_{0,k} - \mathcal{D}^{exp})_r \left(C^{-1}\right)_{rs} (\mathcal{T}_{0,k} - \mathcal{D}^{exp})_s$$

$$C = \Sigma_{PDF} + \Sigma_{stat}$$

- No MC uncertainty.
- Add MC uncertainty corresponding to 10^{10} events.

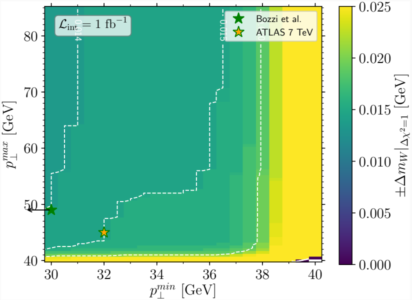

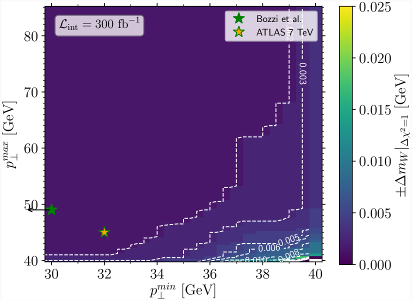

- Large statistics is needed but it does not seem a limiting factor.
-

$$\chi^2_{k,min} = \sum_{(r,s)\in bins} (\mathcal{T}_{0,k} - \mathcal{D}^{exp})_r \left(C^{-1}\right)_{rs} (\mathcal{T}_{0,k} - \mathcal{D}^{exp})_s$$

$$C = \Sigma_{PDF} + \Sigma_{stat} + \Sigma_{MC}$$

- What about other source of uncertainties?

Numerical results: with MC+stat+PDF covariance

- No MC uncertainty.
- Add MC uncertainty corresponding to 10^{10} events.

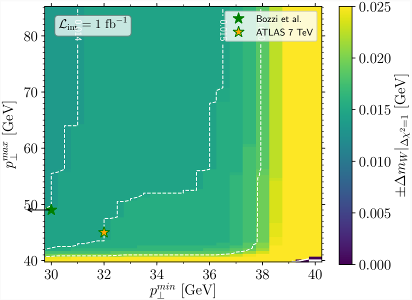

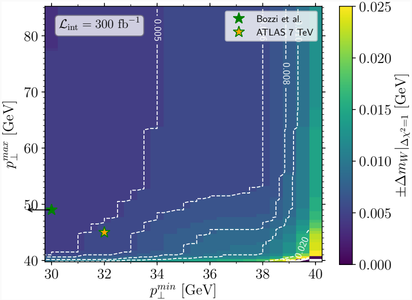

- Large statistics is needed but it does not seem a limiting factor.
-

$$\chi^2_{k,min} = \sum_{(r,s)\in bins} (\mathcal{T}_{0,k} - \mathcal{D}^{exp})_r \left(C^{-1}\right)_{rs} (\mathcal{T}_{0,k} - \mathcal{D}^{exp})_s$$

$$C = \Sigma_{PDF} + \Sigma_{stat} + \Sigma_{MC}$$

- What about other source of uncertainties?

Numerical results: with sys+stat+PDF covariance

- We tried to qualitative understand the impact of detector effects on $p_\perp^l$.
- We used the model proposed by E. Manca (CMS) [CERN-THESIS-2016-173].
- $$\left(\frac{\sigma_{p_T^l}}{p_T^l}\right)^2 = a^2(\eta_l)\cdot r_L^2(\eta_l) + c^2(\eta_l)p^2\cdot r_L^4(\eta_l) + \frac{b^2(\eta_l)\cdot r_L^2(\eta_l)}{1+\frac{d^2(\eta_l)}{p^2}\cdot\frac{1}{r_L^2(\eta_l)}}$$
- Uncertainty of 10^{-4} GeV on the overall muon scale.

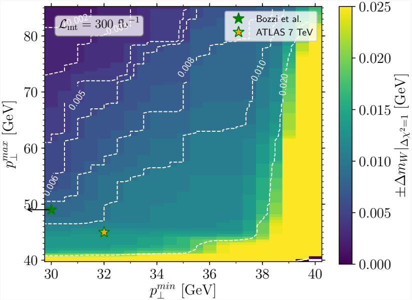

- We compute a "CMS-covariance matrix" using 100 toys. We sum it to the PDF+stat covariance matrix.
- Detector effects reduce the efficacy of the method.
- A quantitative precise statement on the PDF uncertainty depends on the details of the all the systematics of the measurements.

Conclusions and outlook

Conclusions and outlook

Summary

- Treat PDF uncertainty in a frequentist framework as nuisances → covariance matrix.
- Correlation structure of bin above/below the Jacobian peak non-trivial.
- Fitting including the full covariance matrix shows a reduced sensitivity to the PDF uncertainty, if other source of errors are under control.
- Inclusion of bin-bin correlations especially beneficial with large integrated luminosity and good control over the systematics.

Future developments

- What happens to the correlations if we fix the PDF methodology but we change data sets? Disentangle theory vs experimental effects.
- Correlation structure in the other (Hessian) PDF sets.
- Differences between different sets.
- Scale/smearing/MC-modelling dependence of the covariance matrix?